EurJIC
European Journal of Inorganic Chemistry

Communications
doi.org/10.1002/ejic.202000984

Chemistry Europe
European Chemical Societies Publishing

A Facially Coordinating Tris-Benzimidazole Ligand for Nonheme Iron Enzyme Models

Parami S. Gunasekera,[a] Preshit C. Abhyankar,[a] Samantha N. MacMillan,[b] and David C. Lacy*[a]

Herein, we report a new tripodal tris-benzimidazole ligand (**Tbim**) that structurally mimics the 3-His coordination environment of certain nonheme mononuclear iron oxygenases. The coordination chemistry of **Tbim** was explored with iron(II) revealing a diverse set of coordination modes. The aerobic oxidation of biomimetic model substrate diethyl-2-phenylmalonate was studied using the **Tbim**–Fe and Fe(OTf)$_2$.

The mononuclear iron dependent nonheme subclass commonly have an iron center coordinated within a two-histidine one-carboxylate (2-His-1-C) facial triad binding pocket.[1,2] Additional binding modes have also been discovered, and these include the facial three-histidine (3-His), see-saw three-histidine one-carboxylate, and see-saw four histidine binding modes.[3] Modelling of the facial 3-His coordination has been accomplished through various nitrogen donor ligands such as 1,4,7-triazacyclononane (**tacn**),[4] tris(2-pyridyl)methane,[5] trispyrazolyl variants namely trispyrazolylborates,[6] trispyrazolylmethanes[7] and trisimidazolylphosphines (**TIP**).[8] Some of these facially coordinating ligands have been used to prepare Fe-based O_2 derived oxidants, such as superoxo and oxo species[9,10,11,12,13,14] and in catalysis.[15,16]

Despite the successes of these ligands in modeling 3-His coordination,[17,18] we noted that most ligands contain donor groups that are not represented in nature (Figure 1). For instance, histidine donors are aromatic nitrogen groups with sp^2 hybridized N-atoms. In contrast, **tacn** has unconjugated sp^3 hybridization. Accordingly, we noted that facially coordinating ligands with imidazole and benzimidazole N donors have been used to mimic facial 2-His-1-C and 3-His coordination modes with iron.[19,20] Gebbink and coworkers reported a 2-His-1-C facial triad using imidazole and benzimidazole ligands (**2bim1C**) with iron.[19] In another report Fielder and coworkers use **TIP**, which contains imidazole nitrogen donors, to model the 3-His facial triad in an iron complex.[21] It is also noteworthy that, in addition to the electronic similarity (i.e. sp^2 hybridized and aromatized), benzimidazole has excellent pK_a similarities to

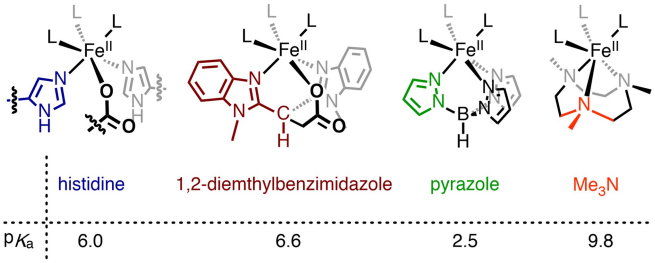

Figure 1. Natural 2H1 C enzyme binding site (left) compared to tridentate ligands with representative "mono-dentate" ligand donor groups and their respective [NH]$^+$ pK_a in water (see Figure S19 and Table S1).

histidine. For example, the pK_a of the nitrogen donor of histidine is 6.0 in water,[22] which is close to the pK_a of 6.6 for 1,2-dimethylbenzimidazole that is the donor moiety in Gebbink's **2bim1C** ligand.[23,24] This is also in contrast to a pK_a of 7.69 for 4-methylimidazole.[25] While differences may be superficial, ligands can impart a certain set of appropriate thermodynamic properties required for dioxygen reactivity.[26] Herein, we report the synthesis of a novel 3-His model with a tris-benzimidazole ligand, 2,2′-(2-(1-ethylbenzimidazol-2yl)ethane-1,1-diyl)bis(1-methylbenzimidazole) (**Tbim**), its coordination with iron, and a brief foray into catalysis.

Synthesis of the new ligand **Tbim** used a strategy inspired by the one Gebbink used to prepare **2bim1C** (Scheme 1).[20,27,28] With ligand in hand, we explored the coordination chemistry of **Tbim** using a variety of FeX_2 salts (X = OAc, Cl, OTf) (Scheme 2

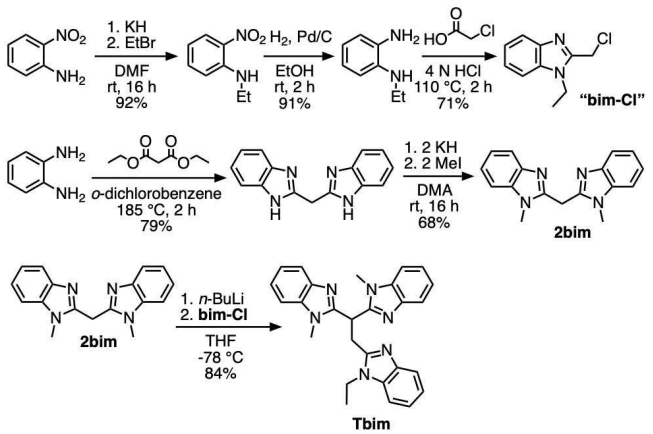

Scheme 1. Ligand synthesis.

[a] P. S. Gunasekera, P. C. Abhyankar, Prof. Dr. D. C. Lacy
Department of Chemistry, University at Buffalo, State University of New York,
Buffalo, New York 14260, United States
E-mail: dclacy@buffalo.edu
[b] Dr. S. N. MacMillan
Department of Chemistry and Chemical Biology, Cornell University,
Ithaca, New York 14853, United States

Supporting information for this article is available on the WWW under https://doi.org/10.1002/ejic.202000984

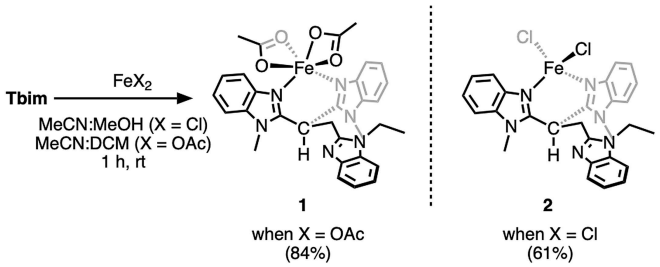

Scheme 2. Synthesis of **1** and **2**.

and Scheme 3). Treatment of **Tbim** with $Fe(OAc)_2$ or $Fe(Cl)_2$ in an acetonitrile solvent mixture afforded new complexes from which crystals suitable for diffraction revealed the mono-ligated complexes [Fe{**Tbim**}$(X)_2$] (**1**, X = OAc; **2**, X = Cl) (Figure 2). The complexes show paramagnetically shifted ^{1}H NMR signals in the range −20 ppm to 90 ppm; Evans method was conducted and is consistent with an S = 2 ground state for **1** and **2** (μ_{eff} = 5.31 and 5.79). Both acetates in **1** are κ-2 and **Tbim** is bound through the two benzimidazole arms that form six-membered chelate rings; the third benzimidazole arm, if bound to the metal, would give a seven-membered ring. Salt metatheses with $NaBPh_4$ on **1** or **2** were performed in MeOH in an attempt to remove a single acetato or chlorido ligand and coordinate the third benzimidazole arm to iron. However, the reaction produced a yellow precipitate from which we obtained colorless crystals of the formulation [Fe{**Tbim**}$_2$][BPh_4]$_2$ ([**3**][BPh_4]$_2$), which is a bis-ligated metal complex salt whose connectivity was confirmed through XRD (Figure S16).

A reaction of **Tbim** with $Fe(OTf)_2$·2MeCN in acetonitrile also produced the bis-ligated metal complex [**3**][OTf]$_2$. However, if a different workup procedure was used for the same *in situ* prepared 1:1 ligand:metal mixture, a different product was obtained. Namely, if the acetonitrile reaction mixture was removed *in vacuo* to near dryness and the resulting residue dissolved in dichloromethane the mono-ligated metal complex [Fe{**Tbim**}$(MeCN)_2$(OTf)][OTf] ([**4**][OTf]) was obtained in moderate yields. The presence of acetonitrile ligands is confirmed from ATR-FTIR spectroscopy (ν_{CN} = 2279 and 2285 cm^{-1}) and X-ray crystallography (Figure 2). Owing to a Schlenk-like equilibrium between the two complexes and free $Fe(OTf)_2$, [**4**][OTf] was inseparable from [**3**][OTf]$_2$ under the conditions studied here.

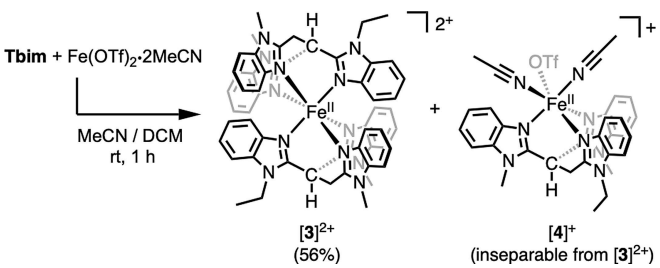

Scheme 3. Synthesis of $[\mathbf{3}]^{2+}$ and $[\mathbf{4}]^{+}$.

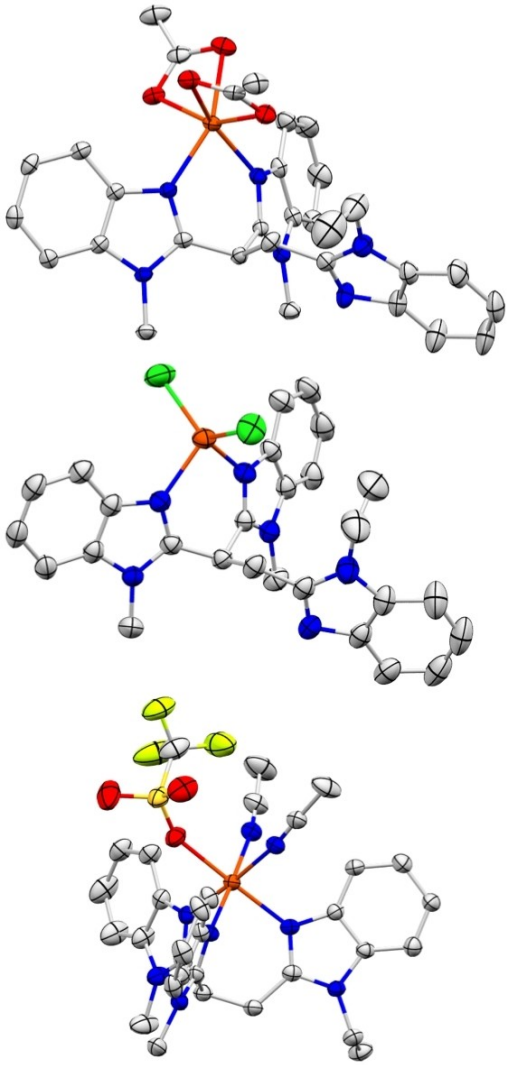

Figure 2. Molecular structure of (top to bottom) **1**, **2** and $[\mathbf{4}]^{+}$ with ellipsoids shown at 50% probability; H-atoms, counterions, and solvent molecules are not shown. Color scheme: orange = Fe; blue = N; red = O; yellow/green = F; yellow = S; green = Cl; grey = C.

A 1:1 reaction mixture of **Tbim** with $Fe(OTf)_2$·2MeCN in acetonitrile followed by ^{1}H NMR and ^{19}F {^{1}H} NMR indicated the presence of both the mono-ligated and the bis-ligated complexes in solution (Figure S15). The ^{19}F {^{1}H} NMR spectrum of a 2:1 ligand:metal ratio contains a sharp peak at −80 ppm consistent with an unbound triflate ion for [**3**][OTF]$_2$.[20] In contrast, when the ratio is less than 2:1, a broad signal is apparent at −73 ppm indicative of an equilibrium between bound and unbound triflate ions in solution implicating the presence of mono-ligated species $[\mathbf{4}]^{+}$ (Figure S12). This is consistent with a Schlenk-like equilibrium between $[\mathbf{3}]^{2+}$ and $[\mathbf{4}]^{+}$ at room temperature in MeCN; using density functional theory (DFT), the calculated equilibrium lies toward the bis-ligated complex with a free energy of −3.2 kcal/mol (see SI). ^{1}H NMR spectroscopy was used to construct a kind of "Job plot" to determine the optimal ratio of $Fe(OTf)_2$:**Tbim** to prepare *in situ* $[\mathbf{4}]^{+}$ for the catalysis studies later (Figure S17), the optimal ratio

to achieve the highest concentration of $[\mathbf{4}]^+$ in the 10 mM regime was found to be 3:2.

In nature, Fe(II) centers coordinated by the three-histidine facial triad nominally occupy the face of a pseudo octahedron similar to the coordination observed in $[\mathbf{4}]^+$ (Figure 3). However, there are some notable differences between $[\mathbf{4}]^+$ and enzymatic coordination. The average benzimidazole Fe–N distance of $[\mathbf{4}]^+$ is 2.15 Å (average distance for all Fe–N/O bonds in $[\mathbf{4}]^+$ is 2.16 Å), whereas the average Fe–N/O distance in resting state mammalian cysteine dioxygenase (CDO) determined through K-edge EXAFS is 2.04 Å.[33] Additionally, the protein structures' N–M–N angles are about 98° (average angle 95.7° for 2atf, 100.6° for 2b5 h, 94.5 for 4fbf,[31] and 102.4° for 3bal), whereas $[\mathbf{4}]^+$ has an average N–Fe–N angle of 89.9° for the benzimidazole nitrogen atoms. Also, it is to be noted that, unlike the binding mode in **Tbim** and other synthetic ligands (e.g., **Tp**), the protein active site imidazoles twist into a paddle wheel conformation.

Following from the structural comparison of $[\mathbf{4}]^+$ with 3-His coordination at enzyme active sites, we next tested $[\mathbf{4}]^+$ in biomimetic oxidation reactions and chose the substrate lithium diethyl 2-phenylmalonate (Li[Phmal], or Li[**a**]), a model substrate often used in biomimicry of the 3-His enzyme diketone dioxygenase (Dke1).[15,34] The use of Li[**a**] in Dke1 model studies is common because the natural substrate acac is difficult to oxidize; even Dke1 has a sluggish rate for acac oxidation (k_{cat} = 6.5 s^{-1}).[35] The expected product distribution for aerobic oxidation of diethyl 2-phenylmalonate (H-**a**) has been studied using a system with O_2 and electrochemically generated superoxide.[36] These products are ethylbenzoylformate (**b**) and HOPhmal (**c**) and their relative distribution depends on the concentration of substrate owing to competing reaction paths from a common alkylperoxo intermediate.

Catalytic oxidation studies were performed by treating a solution of Li[**a**] and 5 mol% catalyst with bubbling O_2 for 1 hour (Scheme 4). After an aqueous work-up (see SI) the products were analyzed by GCMS and compared against authentic samples (Figures S20–S24). Under the conditions we used, H-**a** was obtained as the major final product when no catalyst was present. For runs that contained a catalyst a mixture of both **b** and **c** were obtained (Table 1); if water was not rigorously excluded, **c** was obtained as the major product.[37] When the iron triflate control oxidation contained the oxygen radical scavenger diphenylamine,[38] H-**a** was obtained as the major product accompanied by a small amount of **c** indicating that radical oxygen species are responsible for the oxidation. However, KO_2 (either with or without O_2) did not oxidize Li[**a**] under the parent conditions we used (Scheme 4).

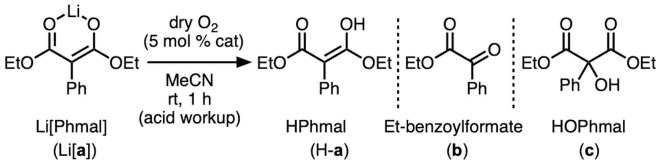

Scheme 4. Catalytic 1,3-Diester Oxidation Studies.

Table 1. Results from catalytic aerobic oxidation of lithium diethyl 2-phenylmalonate (Li[Phmal]).[a]

cat[b]	H-**a** [%]	**b** [%]	**c** [%]
Fe/Tbim (3:2); "$[\mathbf{4}]^+$"	0	22	41
Fe/Tbim(1:4); "$[\mathbf{3}]^{2+}$"	0	17	51
Fe	0	16	41
Fe + Ph_2NH	61	0	17
no iron or ligand	77	0	4

[a] Conditions: Substrate added dropwise, 5 mol% catalyst, dry O_2, 1 h; data reported average of two runs, see SI for full data. [b] **Fe** = Fe$(OTf)_2$·2MeCN; **Fe/L** represents that complex was prepared *in situ*.

In conclusion, we synthesized the biomimetic ligand **Tbim** and prepared coordination complexes with iron that structurally mimics the 3-His active site in nonheme iron enzymes, such as Dke1. We also demonstrated catalytic oxidation chemistry using the substrate Li[**a**], but the simple salt $Fe(OTf)_2$ had comparable performance and so the role of ligand was not inferred. Therefore, despite the common use of Li[**a**], it is not advisable for biomimetic studies where it could give a "false positive" of ligand-induced biomimicry. Novel ligand platforms are still required to achieve the selectivity and rates achieved in enzymes. In particular, designing systems that do not form bis-ligated complexes and can oxidize difficult substrates like acac are required and are ongoing.

Deposition Numbers 1990453 (for **1**), 1990454 (for **2**), and 1990455 (for $[\mathbf{4}]^+$) contain the supplementary crystallographic data for this paper. These data are provided free of charge by the joint Cambridge Crystallographic Data Centre and Fachinformationszentrum Karlsruhe Access Structures service www.ccdc.cam.ac.uk/structures.

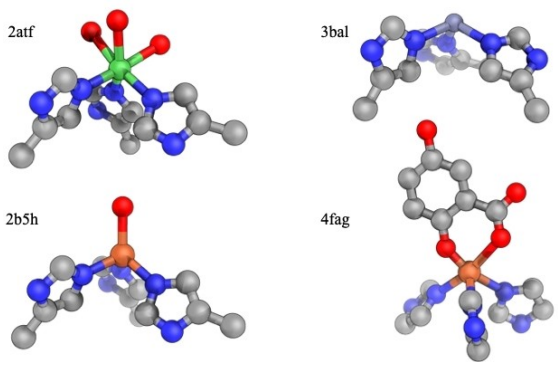

Figure 3. Simplified primary coordination spheres of three-histidine iron enzymes and $[\mathbf{4}]^+$. Clockwise from top left: PDB 2atf (Ni-bound CDO),[29] PDB 3bal (Zn-bound Dke1),[30] 4fag (Fe-bound gentisate dioxygenase),[31] PDB 2b5h (Fe-bound CDO).[32] Color scheme: grey = C; blue = N; red = O; orange = Fe; green = Ni; blue-grey = Zn.

Acknowledgements

Financial support was provided by the University at Buffalo (UB). This work was completed using the resources of the Chemistry Instrument Center (CIC) and Center for Computational Research (CCR) at UB. The FTICR Mass spectrometer used in this study was purchased with funding from NIH S10 RR029517.

Conflict of Interest

The authors declare no conflict of interest.

Keywords: Nonheme iron · Coordination chemistry · Oxygenase · Enzyme model · Ligand design

[1] P. C. A. Bruijnincx, G. Van Koten, R. J. M. K. Gebbink, *Chem. Soc. Rev.* **2008**, *37*, 2716–2744.
[2] K. D. Koehntop, J. P. Emerson, L. Que, *J. Biol. Inorg. Chem.* **2005**, *10*, 87–93.
[3] D. Buongiorno, G. D. Straganz, *Coord. Chem. Rev.* **2013**, *257*, 541–563.
[4] D. W. Blakesley, S. C. Payne, K. S. Hagen, *Inorg. Chem.* **2000**, *39*, 1979–1989.
[5] K. Anandababu, R. Ramasubramanian, H. Wadepohl, P. Comba, N. J. Britto, M. Jaccob, R. Mayilmurugan, *Chem. Eur. J.* **2019**, *25*, 9540–9547.
[6] M. Sallmann, C. Limberg, *Acc. Chem. Res.* **2015**, *48*, 2734–2743.
[7] D. L. Reger, C. A. Little, A. L. Rheingold, R. Sommer, G. J. Long, *Inorganica Chim. Acta*, **2001**, *316*, 65–70.
[8] C. G. J. Tazelaar, J. C. Slootweg, K. Lammertsma, *Coord. Chem. Rev.* **2018**, 356, 115–126.
[9] F. Oddon, Y. Chiba, J. Nakazawa, T. Ohta, T. Ogura, S. Hikichi, *Angew. Chem., Int. Ed.*, **2015**, *54*, 7336–7339.
[10] A. A. Fischer, S. V. Lindeman, A. T. Fiedler, *Chem. Commun.* **2018**, *54*, 11344.
[11] J. B. Gordon, A. C. Vilbert, I. M. DiMucci, S. N. MacMillan, K. M. Lancaster, P. Moëmme-Loccoz, D. P. Goldberg, *J. Am. Chem. Soc.* **2019**, *141*, 17533–17547.
[12] D. Kass, T. Corona, K. Warm, B. Braun-cula, U. Kuhlmann, E. Bill, S. Mebs, M. Swart, H. Dau, M. Haumann, P. Hildebrandt, K. Ray, *J. Am. Chem. Soc.* **2020**, *142*, 5924–5928.
[13] C. W. Chiang, S. T. Kleepspies, H. D. Stout, K. K. Meier, P. Y. Li, E. L. Bominaar, L. Que, E. Münk, W. Z. Lee, *J. Am. Chem. Soc.* **2014**, *136*, 10846.
[14] M. N. Blakely, M. A. Dedushko, P. C. Y. Poon, G. Villar-Acevedo, J. A. Kovacs, *J. Am. Chem. Soc.* **2019**, *141*, 1867–1870.
[15] I. Siewert, C. A. Limberg, *Angew. Chem. Int. Ed.*, **2008**, 47, 7953–7956.
[16] S. Debobrata, T. K. Paine, *Chem. Sci.* **2016**, *7*, 5322–5331.
[17] S. Sahu, D. P. Goldberg, *J. Am. Chem. Soc.* **2016**, *138*, 11410–11428.
[18] L. Que, W. B. Tolman, *Nature* **2008**, *455*, 333–340.
[19] P. C. A. Bruijnincx, M. Lutz, A. L. Spek, W. R. Hagen, B. M. Weckhuysen, G. Van Koten, R. J. M. K. Gebbink, *J. Am. Chem. Soc.* **2007**, *129*, 2275–2286.
[20] P. C. A. Bruijnincx, M. Lutz, A. L. Spek, E. E. Van Faassen, B. M. Weckhuysen, G. Van Koten, R. J. M. Klein Gebbink, *Eur. J. Inorg. Chem.* **2005**, 4, 779–787.
[21] H. Park, J. S. Baus, S. V. Lindeman, A. T. Fiedler, *Inorg. Chem.* **2011**, *50*, 11978–11989.
[22] A. Moser, K. Range, D. M. York, *J. Phys. Chem. B.* **2010**, *114*, 13911–13921.
[23] The pK_a of 1,2-dimethylbenzimidazole was measured as part of this work (see SI).
[24] C. H. R. Martínez, C. Dardonville, *ACS Med. Chem. Lett.* **2013**, *4*, 142–145.
[25] B. Lenarcik, P. J. Ojczenasz, *Heterocyclic Chem.* **2002**, *39*, 287.
[26] D. C. Lacy, *Inorg. Chem. Front.* **2019**, *6*, 2396–2403.
[27] S. Elgafi, L. D. Field, B. A. Messerle, P. Turner, T. W. J. Hambley, *Organomet. Chem.* **1999**, *588*, 69–77.
[28] I. I. Sahay, P. S. Ghalsasi, *Synth. Commun.* **2017**, *47*, 825–834.
[29] J. G. McCoy, L. J. Bailey, E. Bitto, C. A. Bingman, D. J. Aceti, B. G. Fox, G. N. Phillips, *Proc. Natl. Acad. Sci. USA* **2006**, *103*, 3084–3089.
[30] G. R. Stranzl, U. G. Wagner, G. Straganz, W. Steiner, C. Kratky, Protein Data Bank in Europe, https://www.ebi.ac.uk/pdbe/entry/pdb/3bal, (accessed June 2020), unpublished work.
[31] M. Ferraroni, L. Steimer, I. Matera, S. Bürger, A. Scozzafava, A. Stolz, F. Briganti, *J. Struct. Biol.* **2012**, *180*, 563–571.
[32] C. R. Simmons, Q. Huang, Q Hao, T. P. Begley, P. A. Karplus, M. H. Stipanuk, *J. Biol. Chem.* **2006**, *281*, 18723–18733.
[33] S. C. Chai, J. R. Bruyere, M. J. Maroney, *J. Biol. Chem.* **2006**, *281*, 15774–15779.
[34] a) C. J. Allpress, K. Grubel, E. Szajna-Fuller, A. M. Arif, L. M. Berreau, *J. Am. Chem. Soc.* **2013**, *135*, 659–668; b) H. Park, M. M. Bittner, J. S. Baus, S. V. Lindeman, A. T. Fiedler, *Inorg. Chem.* **2013**, *135*, 659–668; c) R. Ramasubramanian, K. Anandababu, M. Kumar, R. Mayilmurugan, *Dalton Tran.* **2018**, *47*, 4049–4053.
[35] G. D. Straganz, B. Nidetzky, *J. Am. Chem. Soc.* **2005**, *127*, 12306–12314.
[36] P. M. Allen, U. Hess, C. S. Foote, M. M. Baizer, *Synthetic Communications* **1982**, *12*, 123–129.
[37] See SI for drying procedure.
[38] P. Comba, Y. M. Lee, W. Nam, A. Waleska, *Chem. Commun.* **2014**, *50*, 412.

Manuscript received: October 23, 2020
Revised manuscript received: November 30, 2020
Accepted manuscript online: December 11, 2020